

Data-driven preliminary dynamics analysis of cranes using rope angle and load measurements

F. P. Candan^{1,*}, S. Canan¹, A. Saday²

¹Elfatek Elektronik, Research and Development Department, Konya, Türkiye

²Faculty of Technology, Department of Electrical-Electronics Engineering, Selçuk University, Konya, Türkiye

ARTICLE INFO

Article Type:

Selected Research Article^c

Article History:

Received: 21 November 2025

Revised: 16 December 2025

Accepted: 19 December 2025

Published: 31 December 2025

Editor of the Article:

M. E. Şahin

Keywords:

Anti-sway,
Crane dynamics,
Fundamental analysis,
Load analysis,
Time series

ABSTRACT

Overhead cranes play a crucial role in industrial operations, yet oscillatory motions during handling tasks may threaten both safety and efficiency. This study proposes a simple but systematic approach for conducting an initial assessment of crane dynamic behavior by jointly analyzing rope angle measurements and load data transmitted via a controller area network (CAN) bus system. The dataset, sampled every five seconds, was cleaned through the removal of missing entries and outliers, followed by descriptive analysis, correlation evaluations, histogram and boxplot inspections, and time-series exploration. The results indicate that the X and Y rope angles exhibit low variability with relatively uniform distributions, while the load data are right-skewed, dominated by low values but occasionally reaching very high magnitudes. A moderate positive relationship was observed between the two angle axes, whereas their associations with load remained weak. Time-series trends and moving-average assessments showed that sudden increases in load can trigger noticeable angular deviations, making the crane more sensitive under heavier operating conditions. Overall, the system demonstrates stable behavior under normal loads, yet risks become more significant as load levels rise. The study aims to outline dominant oscillation components in the frequency domain, establish a reproducible and straightforward data processing workflow, and provide preliminary indicators that may support future anti-sway optimization and predictive maintenance strategies.

Cite this article: F. P. Candan, S. Canan, A. Saday, "Data-driven preliminary dynamics analysis of cranes using rope angle and load measurements," *Turkish Journal of Electromechanics & Energy*, 10(3), pp.118-124, 2025.

1. INTRODUCTION

Overhead cranes play a fundamental role in the safe and efficient handling of heavy loads in industries such as manufacturing, steel processing, energy, and logistics. Overhead cranes are considered safety-critical assets in industrial contexts. Load-sway related incidents can lead to dropped loads, collisions with surrounding equipment, and extended downtime. In many manufacturing plants, a single crane is a bottleneck for the entire production line, so even short interruptions directly translate into productivity losses and maintenance costs [1]. At the same time, modern safety regulations and Conformité Européenne (CE) based design rules require continuous monitoring of overloads and usage profiles. Therefore, there is a strong industrial need for field-validated datasets and simple analysis pipelines that can support anti-sway tuning, condition monitoring, and predictive-maintenance decisions. However, pendulum-like load oscillations pose serious risks to both occupational safety and cycle times; therefore, oscillation prediction, suppression, and motion planning have long been active areas of research in the literature. In recent years, approaches such as input shaping, sliding-mode

control, and observer-based methods have been developed by incorporating variable rope length and double pendulum effects [2-3].

Therefore, it is critical to measure the swing angle accurately, both in control algorithms and in field operations. Studies have shown that swing angles can be estimated in real time using observer-based and filter-based methods, non-contact soft-sensor solutions with acoustic phase-difference approaches, and camera-based visual detection techniques [4]. These solutions, when used in conjunction with swing damping and path-following controls, increase positioning accuracy and safety [5-6].

Data obtained through simultaneous measurements support model-based control approaches, which are prevalent in the literature, with field-appropriate profiles. Recent compilation and application studies comprehensively address two-dimensional and three-dimensional models, base-accelerated pendulum formulations, parameter uncertainty, and hoist (L variation) effects, and suggest combining data-driven approaches with traditional control approaches [7].

^cInitial version of this article was presented at the 6th International Conference of Materials and Engineering Technology (TICMET'25) held on October 6-9, 2025, in Gaziantep, Türkiye. It was subjected to a peer-review process before its publication.

*Corresponding author's e-mail: fatmaperihancandan@gmail.com

On the other hand, data-driven approaches are exploring crane dynamics in the context of model discovery and digital twins. Recently, methods such as genetic programming and the discovery of nonlinear terms through sparse regression have enabled the explanation of unknown dynamics, and contextually aware digital twins on production lines have supported real-time operational decisions. Remote monitoring solutions from major original equipment manufacturers have also brought trends such as usage profiles, alerts, and condition data to the field [8-10].

Preliminary findings suggest that the rope angle tends to increase with load under specific operating conditions, exhibiting a positive correlation and unexpected angular peaks in certain cycles. This approach paves the way for both more informed selection of entry/travel profiles for anti-sway profile optimization and the identification of indicators derived from load/position history for predictive maintenance. These findings are consistent with the industry's data-driven and digital-twin trends [8-9].

This study presents a straightforward and reproducible framework for preliminary analysis of crane dynamics by combining rope angle and load data collected via a CAN bus link under field conditions. Because the dataset was recorded with a 5-second sampling interval, the findings primarily focus on slow components. Sensitivity to high-frequency oscillations is limited. With this constraint explicitly considered, basic statistical summaries (mean, median, standard deviation, distribution histograms, and IQR-based boxplots), Pearson correlation, and scatter plots of the rope angle-load relationship, as well as time series analyses (moving average and low-frequency spectral content), were conducted after removing missing/outlier values.

2. MATERIALS AND METHOD

The dataset used in the proposed study was obtained from sensors integrated into an industrial overhead crane. The system includes a load cell and an angle sensor. The overload control unit (OCS-CU01, Elfatek Elektronik, Konya, Türkiye) is connected to a 10-ton strain-gauge load cell, and the rope-angle limit sensor (ALS-D2C220, Elfatek Elektronik, Konya, Türkiye) provides X and Y rope angles [10].

The load cell measures the lifted mass in kilograms, while the angle sensor records the angle of the rope relative to the vertical axis in degrees. During the dataset creation, measurements were collected at 5-second intervals and recorded over a specific operating period. The dataset used in the study contains approximately 34,155 measurements. Although the overload indicator and rope-angle limit sensor internally operate at approximately 10 Hz (100 ms) sampling rate, the CAN bus measurements analyzed in this study were logged every 5 seconds due to storage and network performance optimization.

The measurements were carried out on an industrial overhead crane equipped with in-house developed monitoring devices. Both the rope-angle limit sensor and the overload control unit are CE-marked and have been tested according to the relevant electrical safety and electromagnetic-compatibility standards. In particular, the rope-angle limit sensor complies with EN 60204-1 (safety of machinery – electrical equipment of machines), EN 61000-6-1 (Electromagnetic Compatibility (EMC) – immunity for residential, commercial and light-industrial environments), EN 61000-6-3 (EMC – emission standard for residential, commercial and light-industrial environments), and EN 60529 (degrees of protection provided by enclosures – IP code). The overload control

unit complies with EN 60204-1:2011, EN 61000-6-1:2007, and EN 61000-6-3:2007/A1:2011 [11-12]. Although the present study does not focus on formal compliance testing, the data were collected under the same safety and EMC conditions as in daily industrial operation.

To improve the reliability of the measurements, both the overload indicator and the rope angle limit sensor were verified and calibrated before sensor data collection. The overload control unit is directly connected to a strain gauge load cell and internally uses a 24-bit HX711-based analog digital converter (ADC) front-end with a 4.3-V reference; this, combined with the device's built-in filtering, provides precise weight resolution throughout the operating range. The unit was calibrated according to the manufacturer's procedure. First, an empty weight operation was performed to subtract the dead weight of the lifting equipment, then a reference test load of at least 25% of the crane capacity was applied and recorded as the calibration point. The rope angle limit sensor uses a dual-axis micro-electro-mechanical systems (MEMS) accelerometer/gyroscope (MPU6050) and provides 1-degree resolution in both X and Y directions. In this study, it was used as a safety-related limit device instead of a high-precision inclinometer. Before collecting the full dataset, a short reference sequence of repeated lift-lower cycles with known loads was recorded three times, and the resulting time series was compared with the crane's onboard gauges and the nominal angle limits configured in the limit sensor. No systematic deviation clearly visible at the scale of the present analysis was observed. During the experiments, both devices cyclically transmitted their measurements over the CAN-open fieldbus, and only CAN frames with valid status information were stored for subsequent statistical and time series analysis.

Before the analysis, various pre-processing steps were applied to the data. First, the time series was examined, and missing observations were identified. Linear interpolation and simple moving average-based smoothing were used to fill in short-term gaps without disrupting the trend and continuity. This approach is frequently used in industrial sensor time series [13]. Especially in short-term data losses, linear interpolation provides continuity without disrupting the actual operating curve. Then, physically impossible values in the measurements were removed. Negative load values or rope angles exceeding 90 degrees were considered to be due to sensor error or recording problems and were removed from the data set. This step is critical for increasing the reliability of the analyses. Fence-based methods, such as the interquartile range (IQR), are used to detect and clean outliers, thereby improving the quality of industrial data [14-15].

After ensuring data integrity, load and rope angles were synchronized using a time stamp. To eliminate time drift between different sensors, all variables were mapped to a common timeline. Load values were normalized by dividing them by the crane's nominal capacity, thus ensuring comparability across different operating conditions. This approach ensured the comparability of records obtained under different operating conditions, allowing for the analysis of the load based on its capacity utilization rate. Methods such as event-based delay estimation for short and noisy sequences are also proposed in the literature [16].

A preliminary data science analysis is presented on rope angle (X, Y; degrees) and load time series obtained from field measurements. The pre-processed dataset contains 3231 timestamped observations. Timestamps are spaced 5 seconds apart, with occasional gaps of 6-10 seconds, thus ensuring approximately uniform sampling.

Following the pre-processing, three fundamental analysis methods were applied to reveal the general characteristics of the data. First, descriptive statistics (mean, median, and standard deviation) were calculated. Second, scatter plots were generated to visualize the relationships between the main variables. Third, correlation analysis was conducted to reveal the relationship between the rope angle and the load. The Pearson correlation coefficient was calculated to determine the strength and direction of the linear relationship between the two variables. The Pearson method has been used as a benchmark for linear relationships in recent studies [17]. Finally, a time series analysis was performed. In this context, the dynamics of angular motions due to load changes were examined, with particular emphasis on oscillatory behavior and periodic components.

Various statistical and visual methods were used in the analysis of the study. Fundamental statistical analyses included the mean and median, standard deviation, histogram for distribution analysis, Pearson correlation, and outlier analysis. Line charts and moving average values were interpreted for time series analysis.

The mean, median, and standard deviation were calculated to determine the central tendency and variation of the rope angle and load variables. The mean and median were evaluated together to examine symmetry or skewness in the distributions. The mean is obtained by dividing the sum of the values of a variable by the number of observations. The median method is defined as the value that divides the ranked data into two equal halves. If the number of observations is odd, the middle value is calculated; if the number of observations is even, the average of the two middle values is calculated. The standard deviation is defined as the square root of the average of the squared deviations of the data from the mean. Before calculating these values, the parameters need to be defined: Equation (1) calculates the mean, which is the average of the data, and Equation (2) calculates the standard deviation, which measures the dispersion of the data from the mean.

$$\bar{x} = \frac{1}{n} \sum_{i=1}^n x_i \quad (1)$$

$$s = \sqrt{\frac{\sum_{i=1}^n (x_i - \bar{x})^2}{n-1}} \quad (2)$$

A histogram visualized the distribution characteristics of rope angles and load. The differences in density and the distribution skew were particularly evident in the load variable. In the histogram method, the data range is divided into equal classes to visualize the data distribution. The number of observations in each class (frequency) is calculated, and these frequencies are displayed in rectangular columns. Equation (3) is used as the basis for mathematical histogram analysis.

$$fre_j = \#\{x_i | a_j \leq x_i < a_{j+1}\} \quad (3)$$

The linear relationship between load and rope angles was measured using Pearson's correlation. The strength and direction of the correlation coefficient were calculated, and scatter plots provided visual support. The Pearson correlation coefficient (r) measures the strength and direction of the linear relationship between two variables. Equation (4) was used as the basis for the calculation.

$$r_{xy} = \frac{\sum(x_i - \bar{x})(y_i - \bar{y})}{\sqrt{\sum(x_i - \bar{x})^2 \cdot \sum(y_i - \bar{y})^2}} \quad (4)$$

Outlier analysis specifically identified extreme values in the load variable. The interquartile range (IQR) method was used in boxplot charts, clearly illustrating deviations from the central tendency. The IQR is calculated by subtracting the first quartile (Q1) from the third quartile (Q3), as shown in Equation (5). In the IQR method, values 25% below the first quartile of the data were calculated, with Q3 representing the values 75% below the data. An observation below the lower limit is defined as an extremely low value, while an observation above the upper limit is defined as an extremely high value [18].

$$\begin{aligned} IQR &= Q3 - Q1 \\ Lower &: Q1 - 1.5 \cdot IQR \\ Upper &: Q3 + 1.5 \cdot IQR \end{aligned} \quad (5)$$

In the line graph method, load and angular values are evaluated together on the time axis. Sudden load increases and accompanying angular deflections are visualized. Each measurement in the line graph displays the corresponding value to the timestamp. This allows us to examine how load and rope angles change over time. Using a moving average, the load and angle series are smoothed out, eliminating short-term fluctuations within a specific window width. This method reduces the impact of short-term fluctuations, making overall trends visible [19]. The moving average is calculated using Equation (6).

$$MA_t = \frac{1}{k} \sum_{i=0}^{k-1} x_{t-i} \quad (6)$$

All these steps aim to both increase the reliability of the data and provide a fundamental quantitative description of crane dynamics. This methodological framework provides a solid starting point for future, more complex modeling, simulation, and control studies.

3. RESULTS AND DISCUSSION

Descriptive statistics were calculated for the load and rope angles, including the mean, median, and standard deviation. The mean value for rope angle X is very close to zero, indicating that horizontal deviations are generally balanced. The low standard deviation also confirms this balance. For rope angle Y , the mean is positive, and the median is approximately 1 degree. This indicates that the system operates with small positive deviations most of the time. The mean load is 152.8 kg, whereas the median is only 4 kg. This reveals that the distribution is severely skewed to the right. The high standard deviation also indicates excessive variability in the load. These findings suggest that the system operates primarily with low loads, but occasionally with high loads. The graph of the mean, median, and standard deviation calculations for load and rope angles is presented in Figure 1.

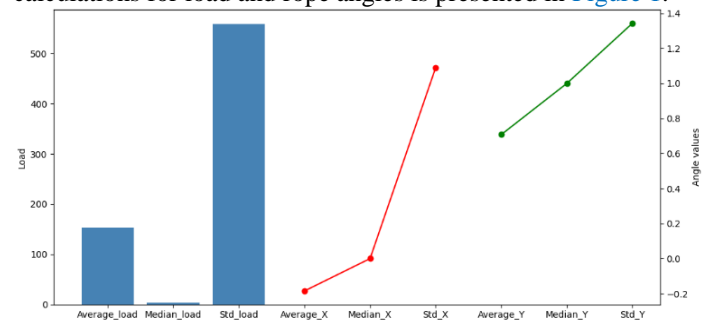


Fig. 1. Mean, median, and standard deviation.

Statistical analysis revealed that the load data averaged 152.8 (≈ 153 kg), and the rope angle generally varied between -4 degrees and 4 degrees. Standard deviation of approximately 559 kg indicates a highly variable load profile, especially during high-load operations. The results of the fundamental analysis are presented in Table 1.

Table 1. Fundamental analysis results.

| Metric | Rope Angle X (deg) | Rope Angle Y (deg) | Load (kg) |
|-------------|-----------------------|-----------------------|--------------|
| Min | -8.0 | -6.0 | 0.0 |
| Max | 3.0 | 7.0 | 3441.0 |
| Mean | -0.18477 | 0.70783 | 152.81616 |
| Std | 1.08971 | 1.34330 | 559.53183 |
| Ptp (range) | 11 | 13 | 3441 |

In the histogram analysis of the study, the rope angle histograms showed a narrow and symmetric distribution, with values mainly concentrated around -1 degree and 1 degree. The load of the histogram, however, was skewed. Low load values were observed frequently, while high load values were observed rarely. This suggests that the typical behavior of the system is based on carrying low loads; however, loads close to capacity are also utilized in critical operations. The histogram of the load and rope angle data in the data set is shown in Figure 2(a-c).

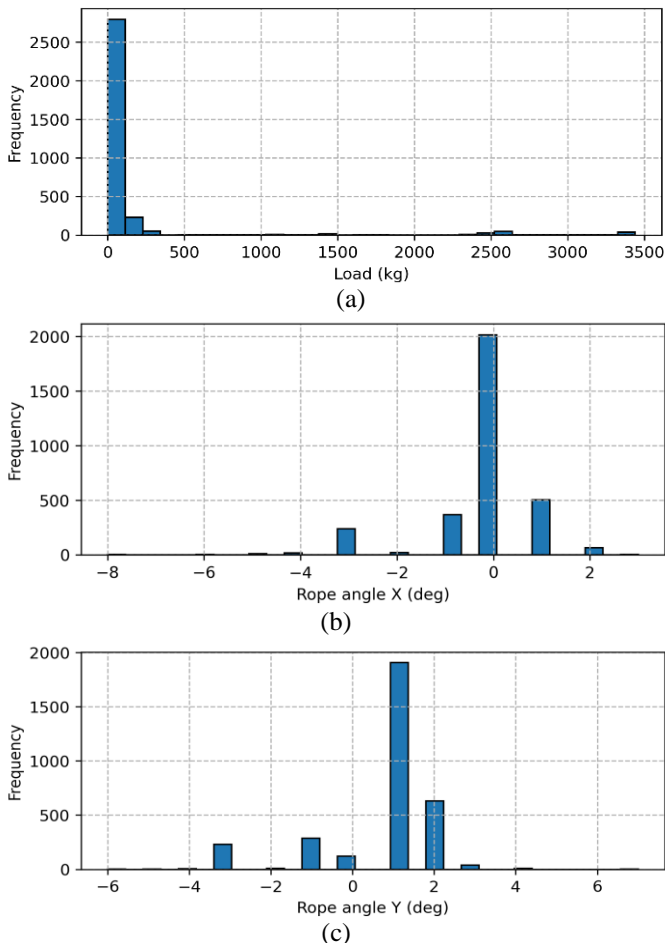


Fig. 2. Histogram-based distribution of crane dataset: (a) load (kg), (b) rope angle X (deg), (c) rope angle Y (deg).

The correlation analysis performed revealed a positive relationship between the load and the rope angle. The tendency for the rope angle to increase as the load increases demonstrates that the dynamic effects of the load become more pronounced. It visually confirms that angular deflections tend to increase as the load increases. This finding demonstrates that the risk of oscillation increases in high-load operations and that the load directly affects the angles in crane dynamics. The scatter plot for the load data is shown in Figure 3(a), and the scatter plot for the rope angles is shown in Figure 3(b) and in Figure 3(c). The correlation matrix for the distribution is shown in Figure 4.

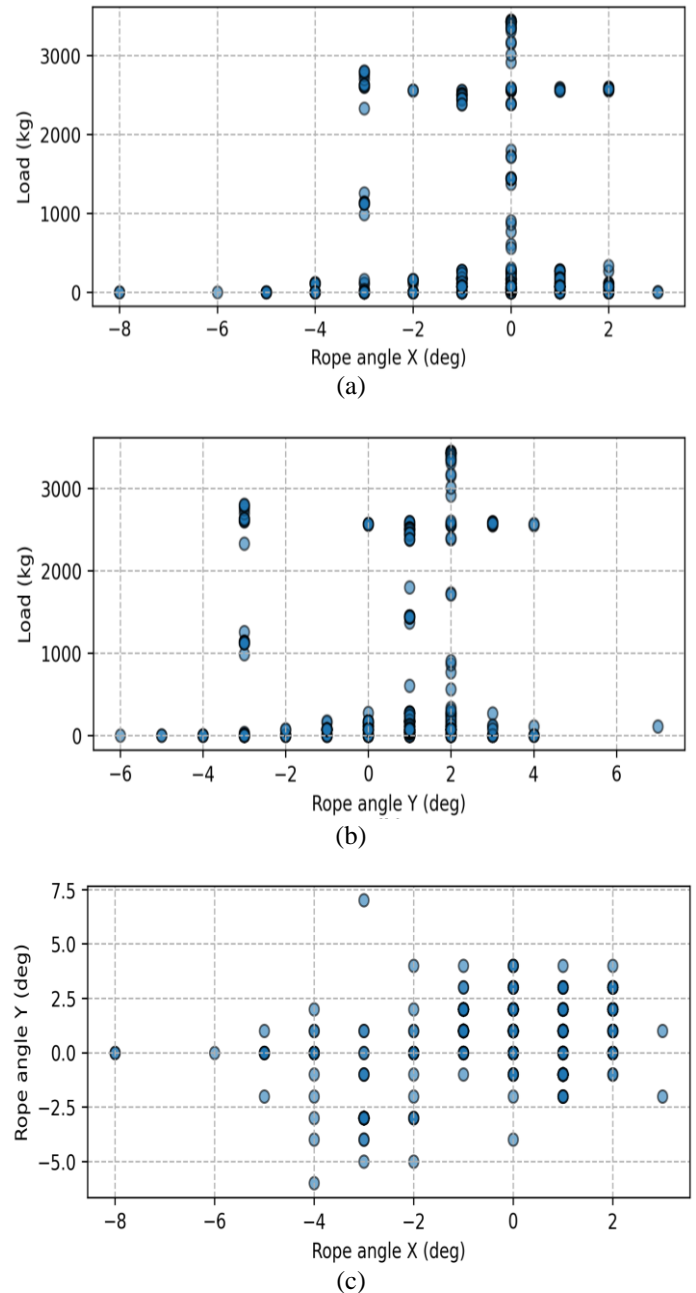


Fig. 3. Scatter plots of the relationships between the main variables: (a) rope angle X vs. load, (b) rope angle Y vs. load, (c) rope angle X vs. rope angle Y.

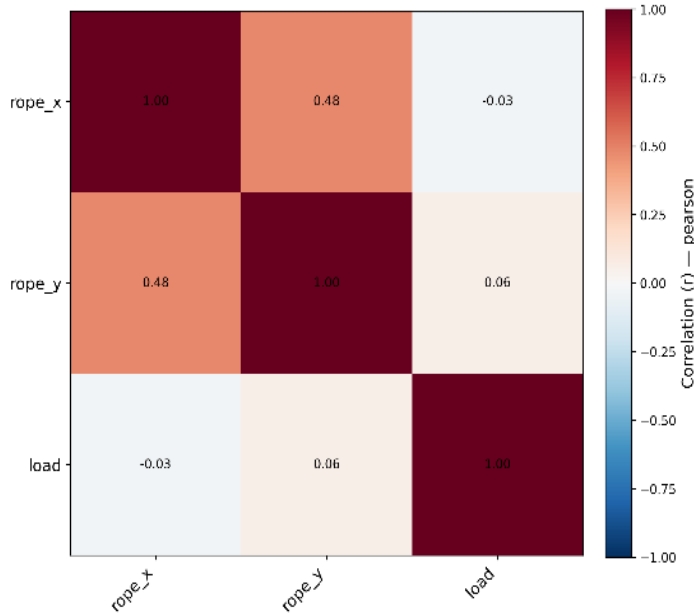


Fig. 4. Rope angle and load correlation matrix of the distribution.

Correlation analysis results were conducted to examine the linear relationships between rope angles (rope_x and rope_y) and load. The resulting correlation matrix shows a moderately positive correlation ($r = 0.48$) between rope_x and rope_y. This suggests that rope angles tend to vary in a dependent manner. However, the correlation coefficient between rope_x and load was found to be -0.03 , and between rope_y and load was found to be 0.06 . Both coefficients are statistically low. Consequently, while load variation may be related more to nonlinear factors or different system parameters, the rope angles exhibit a specific correlation among themselves.

Based on the outlier analysis, extreme values in the load variable were identified. The interquartile range (IQR) method was used in the boxplot graphs, clearly illustrating deviations from the central tendency. Boxplots for load and X, Y angles are shown in Figure 5(a-c), respectively.

When the statistical distributions of the rope_x and rope_y columns were examined in the outlier analysis performed on the variables, it was observed that both variables had minimal variance. The boxplot illustrates the distribution of the load variable. The quartile values were calculated as explained in Section II. The box represents the interquartile range (IQR), spanning from the first quartile (Q1) to the third quartile (Q3). The orange line inside the box indicates the median value. For the rope_x variable, the first quartile (Q1) and third quartile (Q3) values were found to be 0.00, and therefore, the IQR value was equal to 0.00. Similarly, for the rope_y variable, the Q1 and Q3 values were 1.00, and the IQR = 0.00. An IQR of zero indicates that the variable primarily consists of a single fixed value. In contrast, a more significant distribution was observed for the load variable. The Q1 value was 2.00, the Q3 value was 74.00, and the IQR = 72.00. This indicates that the variable has a statistically heterogeneous structure. The lower bound was set at -106.00 , and the upper bound was 182.00 ; the 215 observations falling outside these limits were defined as outliers.

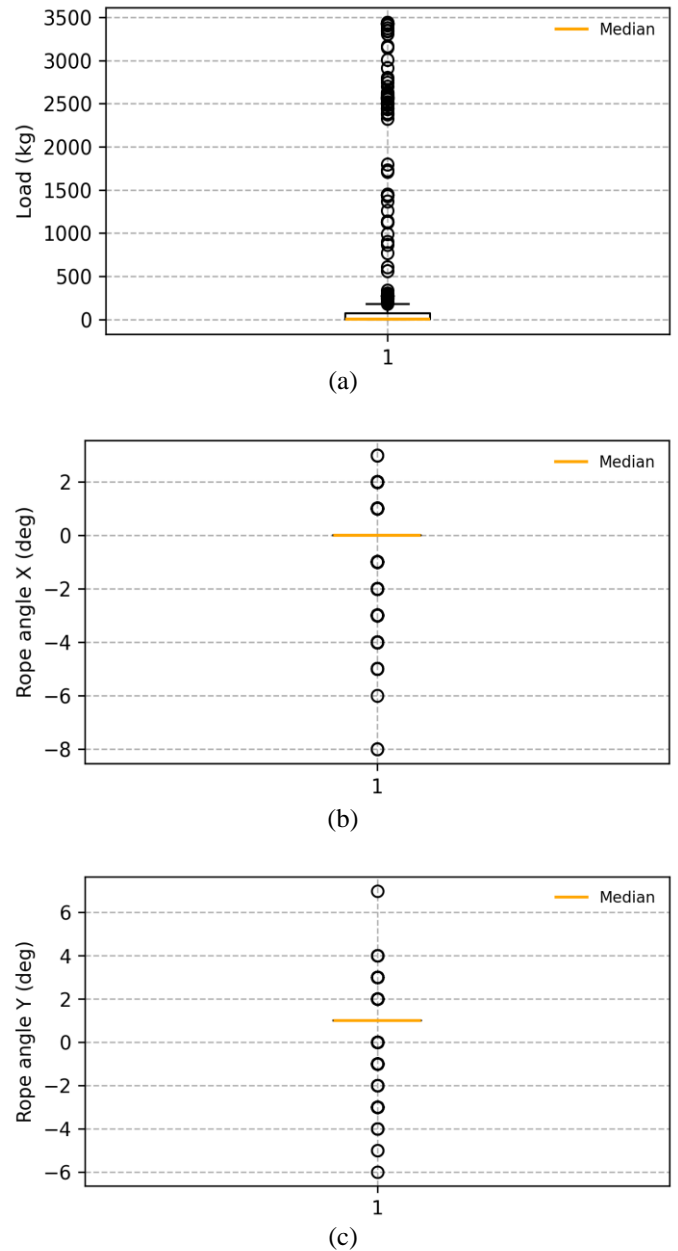


Fig. 5. Boxplots of the main variables based on the IQR method: (a) load (kg), (b) rope angle X (deg), (c) rope angle Y (deg).

In this study, line charts and moving average methods were examined together for time analysis. In the line chart analysis, the load in the time series was mostly low. However, sudden and high load increases were observed at specific time points. During these sudden loads, deviations in the rope angles occurred. The Y angle, in particular, appeared more sensitive to these increases. In the moving average analysis, the method smoothed out short-term fluctuations, revealing the overall trend of the system more clearly. This method more clearly observed that sudden load increases caused simultaneous increases in the angular series. The line chart and moving average graphs obtained from the data are presented in Figure 6(a-c).

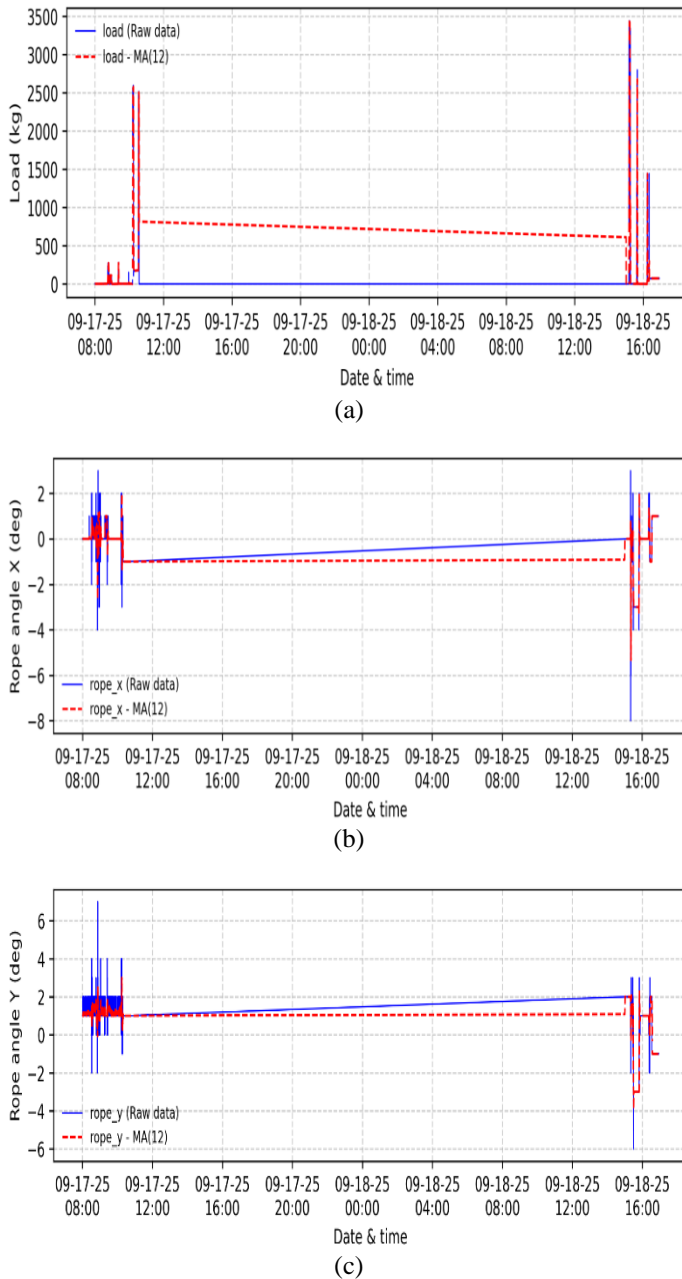


Fig. 6. Load and X–Y rope angle time-series with moving-average curves: (a) load (kg), (b) rope angle X (deg), (c) rope angle Y (deg).

The findings are consistent with the behavior predicted by theoretical models and guide practical applications. The results indicate that the crane system from which the data used in the study were collected generally operated in balance, with low variance in angular deflections, but that extreme values in the load distribution critically affected the system behavior. The fact that sudden load increases cause oscillations in rope angles is a significant issue for operational safety. The pronounced angular increase, particularly at high loads, is a critical finding for operational safety. This preliminary analysis provides a solid foundation for future frequency analysis, advanced modeling, and control strategies.

Compared with recent modeling-oriented studies [1–3, 7], which typically rely on high-frequency measurements or laboratory experiments, our dataset is relatively coarse (5-s sampling) and was collected under real production constraints. This partly explains why the linear correlations between load and angles remain weak ($|r| < 0.1$), whereas the angles themselves exhibit a clear mutual correlation. In practice, the crane operates most of the time at low loads, and with conservative operator behaviour, so large oscillations mainly appear in short, high-load episodes. These features are not always visible in idealized simulation studies but are critical for tuning anti-sway profiles and usage-based maintenance thresholds.

4. CONCLUSION

Comprehensive statistical analyses were conducted on the load and rope angles in the crane system. After removing missing and erroneous data, statistical evaluations revealed a significant relationship between the load and rope angle. Descriptive statistics revealed that the rope angles X and Y generally balanced around small values, while the load variable exhibited a severely right-skewed distribution. In particular, the relatively low median and high mean values in the load data indicate that the system operates mostly with low loads but occasionally encounters high loads.

Correlation analysis revealed a moderately positive relationship between rope angles, while the relationships between load and angles were relatively weak. Scatter plot analysis supported this finding, demonstrating that the relationship between rope angles was somewhat scattered rather than linear. Boxplot analyses revealed numerous high-value outliers, particularly for the load variable, while limited variance and low deviations were noted for rope angles.

Time series analyses and moving averages revealed that simultaneous oscillations in rope angles occur in conjunction with sudden load increases. This indicates that system dynamics become more sensitive, particularly during high-load operations, posing critical risks to operational safety.

Overall, the findings indicate that angular misalignments are generally low; however, occasional high loads have a significant impact on system behavior. This study serves as a starting point for more comprehensive research on improving the safety and efficiency of crane operations. Digital twin-based simulations, in particular, provide a valuable database and methodological framework for predictive maintenance strategies and advanced control algorithms.

References

- [1] X. Wang, Z. He, C. Liu, and W. Du, "Anti-sway adaptive fast terminal sliding mode control based on the finite-time state observer for the overhead crane system," *Electronics*, 13(23), p.4709, 2024.
- [2] S. M. F. Rehman et al., "Input shaping with an adaptive scheme for swing control of tower cranes under varying cable lengths," *Ocean Engineering*, 175(111640), August 2022.
- [3] S. Arabasi and Z. Masoud, "Frequency-Modulation Input-Shaping Strategy for Double-Pendulum Overhead Cranes Undergoing Simultaneous Hoist and Travel Maneuvers," *IEEE Access*, vol. 10, pp. 44954-44963, 2022.

- [4] F. Kawai et al., "Observer-based control design for overhead crane systems," *IFAC-PapersOnLine*, 56(2), pp. 2151–2156, 2023.
- [5] H. Ogawa et al., "Improved estimation of sway-angle for overhead crane using phase difference of acoustic signals," *ICAROB2021*, pp. 129–132, Japan, 21-24 January 2021.
- [6] N. Masayoshi et al., "Soft sensor for sway angle of overhead crane using phase difference of acoustic signals," *The 46th Annual Conference of the IEEE Industrial Electronics Society*, pp. 736-741, Singapore, 18-21 October 2020.
- [7] M. R. Mojallizadeh, B. Brogliato and C. Prieur, "Modeling and control of overhead cranes: A tutorial overview and perspectives," *Annual Reviews in Control*, 56(3), p.100877, 2023.
- [8] T. Kuszniir et al., "Data-driven identification of crane dynamics using grammar-guided genetic programming with sparse regression," *Applied Sciences*, 14(8), p. 3492, 2024.
- [9] C. Yang et al., "A digital-twin-driven industrial context-aware system: A case study of overhead crane operation," *Robotics and Computer-Integrated Manufacturing*, 88(102708), pp. 394-409, 2025.
- [10] Elfatek Elektronik, "Vinç Güvenlik Ekipmanları", 2025, www.elfatek.com.tr/vinc-guvenlik-ekipmanlari, [Accessed: 21 Nov. 2025].
- [11] International Electrotechnical Commission, "IEC 60204-1:2016 RLV," 2016, [Online Available]: webstore.iec.ch/en/publication/26036, [Accessed 21 Nov. 2025].
- [12] International Electrotechnical Commission, "IEC 60204-1:2016 RLV," 2016, [Online Available]: webstore.iec.ch/en/publication/26036, [Accessed 21 Nov. 2025].
- [13] A. Flores, H. Tito-Chura, O. Cuentas-Toledo, V. Yana-Mamani, and D. Centty-Villafuerte, "PM2.5 time series imputation with moving averages, smoothing, and linear interpolation," *Computers*, 13(12), 2024.
- [14] C. S. K. Dash, S. Sahu, and J. Nayak, "An outliers detection and elimination framework in data pre-processing stage," *Discover Data*, 3(4), 2023.
- [15] A. S. Alsalehy, Y. Alghofaili, and A. Almkhli, "Improving time series data quality: Identifying outliers and optimization of imputation accuracy," *Informatics*, 8(3), pp. 82, 2025.
- [16] C. Schranz, S. Mayr, S. Bernhart, and C. Halmich, "Nearest advocate: A novel event-based time delay estimation algorithm for multi-sensor time-series data synchronization," *EURASIP Journal on Advances in Signal Processing*, 2024(46), pp.1-24, 2024.
- [17] J. Wu, N. Li, Y. Zhao, and J. Wang, "Usage of correlation analysis and hypothesis test in optimizing the gated recurrent unit network for wind speed forecasting," *Energy*, 242(122960), 2022.
- [18] A. S. AlSalehy and M. Bailey, "Improving time series data quality: Identifying outliers and handling missing values in a multilocation gas and weather dataset," *Smart Cities*, 8(3), p.82, 2025.
- [19] R. J. Hyndman and G. Athanasopoulos, *Forecasting: Principles and Practice*, OTexts, 2018.

Biographies



Fatma Perihan Candan works as a Research and Development Engineer at Elfatek Elektronik. She received her bachelor's degree in Electrical and Electronics Engineering from Necmettin Erbakan University in 2019. She has been involved in R&D processes with a focus on embedded systems, industrial electronics, and communication infrastructures, taking responsibilities in both hardware and software development phases. She has experience in Embedded C, microcontroller-based systems, basic industrial communication protocols, PCB design tools, and testing and validation approaches.

E-mail: fatmaperihancandan@gmail.com



Süleyman Canan completed his undergraduate education in Electrical and Electronics Engineering at Hacettepe University and obtained his Master's and PhD degrees from Selçuk University in 2006. He began his academic career as a Research Assistant at Selçuk University in 1995, and later worked as a Senior Research Engineer at TÜBİTAK Marmara Research Center (1999–2010), where he carried out research and project activities for many years. During this period, he was a visiting researcher at Newcastle University (UK) between 1999 and 2000. Since 2010, he has been managing R&D, technology development, and commercialization-oriented activities as a co-founder of Elfatek Elektronik Ltd.

E-mail: suleyman.canan@elfatek.com.tr



Abdulkadir Saday completed his undergraduate education in Electrical and Electronics Engineering, and obtained his Master's and PhD degrees at Selçuk University in 2024. He began and continues his academic career as a faculty member at Selçuk University, during which he has conducted research and project activities in the fields of embedded systems, FPGA-based designs, artificial intelligence applications, image processing, and robotic systems. His research mainly focuses on embedded artificial intelligence and hardware-based intelligent systems.

E-mail: asaday@selcuk.edu.tr